we obtain $gBH_1 \sim 4\times10^{-2}$ cm^{-1}, so that these two estimates of the strain splitting agree.

A more exacting test of our proposed model would be provided by a precise determination of the quadrupole splitting in the presence of an applied magnetic field. As we found in Sec. VI, when **H** is along [100] the splitting of the $J_z=\pm1$ spectrum equals $+(\frac{3}{2})c_3$, while for **H** along [111] it equals $+2c_5$, so that these parameters, including their signs, may be determined independently. Since c_3 is given by the crystal-field model to be negative and c_5 positive (for Q positive[22]), the sign of the splitting should change as **H** is rotated from [100] to [111]. Any departure in the ratio c_3/c_5 from that given by Eq. (3) would give a measure of the importance of departures from the crystal-field model, such as those that may arise from Jahn-Teller effects.

[22] A. Abragam and F. Bouton, Compt. Rend. **252**, 2404 (1961); G. Burns, Phys. Rev. **124**, 524 (1961).

ACKNOWLEDGMENTS

The author wishes to thank R. B. Frankel, N. A. Blum, and D. N. Pipkorn for communicating their results prior to publication, and he is grateful to the above and also to M. Blume for very helpful discussions of this problem.

PHYSICAL REVIEW VOLUME 160, NUMBER 2 10 AUGUST 1967

Nuclear Magnetic Resonance and Nonexponential Spin-Lattice Relaxation in Ferroelectric Ammonium Fluoroberyllate*

D. E. O'Reilly, E. Mark Peterson, and Tung Tsang
Argonne National Laboratory, Argonne, Illinois

(Received 3 March 1961)

Nuclear spin-lattice relaxation times T_1 and relaxation times along the rf field ($T_{1\rho}$) have been measured for H^1 and F^{19} in $(NH_4)_2BeF_4$. Below 250°K the relaxation is due to reorientation of NH_4^+ ions; proton T_1 versus T has two minima due to two inequivalent NH_4^+ ions in the unit cell. Above the transition temperature T_c (176°K) and below 130°K, the logarithm of the correlation time τ_c is a linear function of T^{-1} with normal values of pre-exponential factors. Immediately below T_c, the time τ_c is anomalously short, as found previously in $(NH_4)_2SO_4$. Above 250°K, both proton and F^{19} relaxation become nonexponential and may be characterized by the same pair of relaxation times T_1' and T_1''. The shorter component (T_1') is ascribed to H-F dipolar interactions, and the longer component (T_1'') to H-F, H-H, and Be-F dipolar interactions. On deuteration, only the longer component remains; also, T_1' and T_1'' depend only on the rate of reorientation of BeF_4 tetrahedra. Deuteron-resonance results indicate that the dipole moment per NH_4^+ ion in $(NH_4)_2BeF_4$ is about half that in $(NH_4)_2SO_4$, in agreement with spontaneous-polarization measurements. The phase transition in $(NH_4)_2BeF_4$ is not as abrupt as in $(NH_4)_2SO_4$, and may be described by a weaker dependence of the interaction parameter on the spontaneous polarization.

I. INTRODUCTION

THE crystal structures of ammonium fluoroberyllate and ammonium sulfate are very similar, and both are known to be ferroelectric; but many differences between those two crystals have also been found.[1,2] By precise x-ray studies, it was found that the crystal symmetries are different in both their room- and low-temperature phases. The axes of polarization in the ferroelectric phases are not in the same crystallographic direction. The phase transition in $(NH_4)_2SO_4$ is first-order and very abrupt, while the transition in $(NH_4)_2BeF_4$ is more gradual.

In view of the similarities and also the differences of these two crystals, both the deuteron magnetic resonance and nuclear magnetic relaxation of H^1 and F^{19} in $(NH_4)_2BeF_4$ have been studied in some detail. The natures of the ferroelectricity and molecular motions will be compared with previous results[3] on $(NH_4)_2SO_4$ deduced from magnetic resonance studies. In addition, molecular motions of BeF_4 ions can be deduced from F^{19} nuclear resonance studies; whereas, similar studies on sulfate ions would be very difficult. By measuring both spin-lattice relaxation time T_1 and the relaxation time $T_{1\rho}$ in the rotating coordinate system, it is possible to observe the molecular motions over wide ranges of correlation times.

In the present work, it was also found experimentally that the nuclear spin-lattice relaxation becomes markedly nonexponential over certain temperature ranges; the relaxation processes have been studied and interpreted in some detail in Sec. IIIB. Although deviations from exponential behavior have been observed and predicted[4] for certain systems, the deviations are very

* Based on work performed under the auspices of the U. S. Atomic Energy Commission.

[1] S. Hoshino, K. Vedam, Y. Okaya, and R. Pepinsky, Phys. Rev. **112**, 405 (1958).

[2] Y. Okaya, K. Vedam, and R. Pepinsky, Acta Cryst. **11**, 307 (1958).

[3] D. E. O'Reilly and T. Tsang, J. Chem. Phys. **46**, 1291 (1967)

[4] I. Solomon, Phys. Rev. **99**, 559 (1955); P. S. Hubbard, *ibid.* **109**, 1153 (1958).

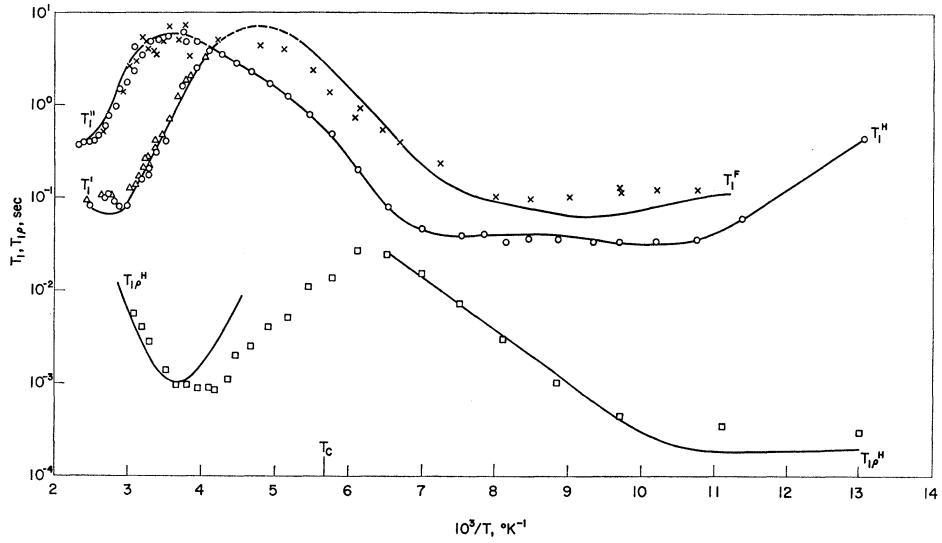

FIG. 1. T_1 and $T_{1\rho}$ data for H^1 and F^{19} in polycrystalline $(NH_4)_2BeF_4$ at 42 Mc/sec and $H_1=16$ G, versus inverse temperature. Protons: T_1, ⊙; $T_{1\rho}$, ⊡. T_1 for F^{19}: △, ×. The solid curves are calculated from correlation times given in Fig. 3.

slight. For $(NH_4)_2SO_4$, which contains protons at two chemically inequivalent sites at which relaxation processes are different, only exponential relaxation is observed because of spin-exchange processes.[3]

II. EXPERIMENTAL PROCEDURE

Proton and fluorine spin-lattice relaxation times (T_1) were measured by the 180°–90° pulse sequence[5a] at 42 Mc/sec using a NMR Specialties (New Kensington, Pennsylvania) model PS-60A pulsed spectrometer, Varian Associates 12-in. electromagnet and variable temperature apparatus. Relaxation times along the rf field ($T_{1\rho}$) were measured by a 90° pulse followed by a pulse shifted 90° in phase and of variable time duration.[6]

Deuteron magnetic resonance was observed near 5 Mc/sec using a conventional Varian Associates V4200B nuclear induction spectrometer, 12-in. electromagnet, and variable-temperature apparatus; the magnetic field was monitored by the proton resonance on a Harvey–Wells NMR gaussmeter. The crystals were rotated about the twofold axes[1] a, b, c; and the quadrupolar coupling tensor was determined by the Volkoff method.[7]

Crystals of $(ND_4)_2BeF_4$ were grown after multiple recrystallization from 99.8% D_2O by slow cooling and evaporation of seeded solutions. The crystal orientations were determined by x-ray diffraction and dielectric constant measurements. A sample of polycrystalline $(ND_4)_2BeF_4$ for F^{19} relaxation-time measurements was prepared by dissolving the solid in D_2O and evaporating to dryness. This procedure was repeated four times and the sample was then dried in vacuum. The proton Bloch decay signal from the deuterated sample was a factor of fifty weaker than the corresponding signal from $(NH_4)_2BeF_4$.

III. PROTON AND FLUORINE RELAXATION-TIME RESULTS

The experimental proton and fluorine relaxation times of polycrystalline $(NH_4)_2BeF_4$ are summarized in Fig. 1 as a semilogarithm plot versus inverse temperature.

The spin-lattice relaxation times T_1 show a rather unusual temperature dependence and are only in approximate agreement with the limited data of Miller, Blinc, Brenman, and Waugh.[8] Above −20°C, the spin-lattice relaxations of both F^{19} and H^1 become strongly nonexponential and are characterized by two relaxation times; a typical semilogarithm plot of $(M_0-M)/M_0$ versus time is given in Fig. 2 for both H^1 and F^{19} at 25°C, where M is the nuclear magnetization along the magnetic field direction and M_0 is the equilibrium value of M. The nonexponential behavior is not an anisotropic effect, since two relaxation times were also observed for a $(NH_4)_2BeF_4$ single crystal with $\mathbf{H} \parallel b$.

The second moment (M_2) of protons[9] in polycrystalline $(NH_4)_2BeF_4$ indicates that all ammonium tetrahedra are reorienting rapidly, with a correlation time τ_c less than 10^{-5} sec, even at −180°C, the lowest experimental temperature. No linewidth transition was observed between 25 and −180°C. On the other hand, a sharp transition occurred for the F^{19} second moment[10] near −60°C because of the reorientation of BeF_4 tetrahedra; τ_c is approximately 10^{-5} sec at that temperature. The BeF_4 tetrahedra are therefore much less mobile than the ammonium ions.

[5] A. Abragam, *The Principles of Nuclear Magnetism* (Oxford University Press, New York, 1961); (a) p. 64, (b) p. 123, (c) pp. 270–296, (d) p. 456 [Eqs. (68) and (68′)], and (e) p. 518.
[6] D. C. Look, I. J. Lowe, and J. A. Northby, J. Chem. Phys. **44**, 3441 (1966); P. S. Hubbard, Rev. Mod. Phys. **33**, 249 (1961).
[7] G. M. Volkoff, H. E. Petch, and D. W. L. Smellie, Can. J. Phys. **30**, 270 (1952).
[8] S. R. Miller, R. Blinc, M. Brenman, and J. S. Waugh, Phys. Rev. **126**, 528 (1962).
[9] R. Blinc and I. Levstek, J. Phys. Chem. Solids **12**, 295 (1960).
[10] G. Burns, Phys. Rev. **123**, 64 (1961).

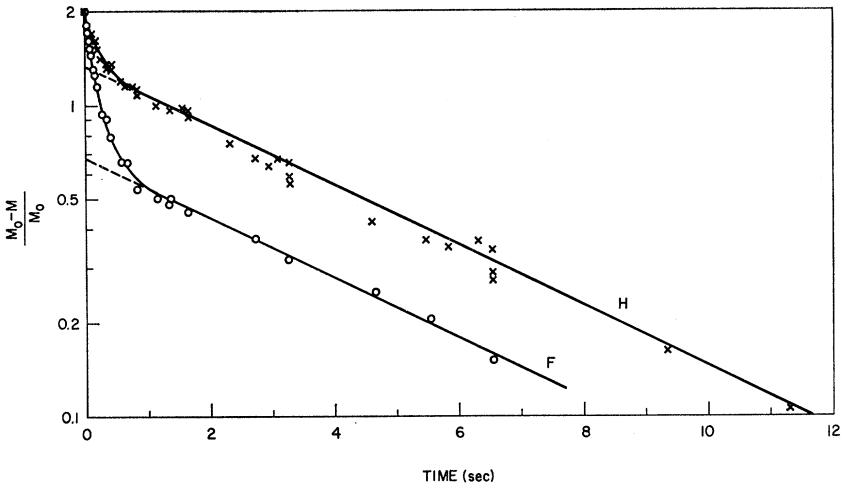

FIG. 2. Semilogarithmic plot of $(M_0-M)/M_0$ versus time (sec) for F^{19} (circles) and protons (crosses) in polycrystalline $(NH_4)_2BeF_4$ at 42 Mc/sec and 25°C. The solid curves are calculated from Eqs. (18) and (19), using $T_1'=0.20$ and $T_1''=4.5$ sec.

It is well known[5c] that T_1 minima occur when $\omega\tau_c$ is approximately unity, ω being the rf frequency. The high-temperature (near $10^3/T=3$ deg^{-1}) and low-temperature (near $10^3/T=9$ deg^{-1}) T_1 minima can therefore be associated with the BeF_4^{2-} and NH_4^+ ion reorientations, respectively. The broad proton T_1 minima between $10^3/T=7$ and 11 can be interpreted as due to two types of NH_4 tetrahedra rotating at different frequencies and coupled to each other via the dipole–dipole interaction; the situation is quite similar[3] to $(NH_4)_2SO_4$, and will be discussed in Sec. IIIA. Spin-lattice relaxation associated with BeF_4 reorientation is discussed in Sec. IIIB, where an explanation for nonexponential relaxation is proposed. In Sec. IIIC, we show that the $T_{1\rho}$ data are consistent with our interpretation of the T_1 results. Additional measurements on $(ND_4)_2BeF_4$ are given in Sec. IIID.

A. Low-Temperature T_1 Data for $(NH_4)_2BeF_4$

For $10^3/T>4$, the proton spin-lattice relaxation time T_1^H is determined mainly by the ammonium-ion reorientation mechanism; the contribution from H-F dipole interactions is quite small. Here we may use the $(NH_4)_2SO_4$ results directly[11] for T_1^H:

$$(T_{1,N}{}^H)^{-1}=(1.3\times10^{10})\left[\frac{\tau_N}{1+\omega^2\tau_N{}^2}+\frac{4\tau_N}{1+4\omega^2\tau_N{}^2}\right], \quad (1)$$

$$2(T_{1,\mathrm{obs}}{}^H)^{-1}=(T_{1,\mathrm{I}}{}^H)^{-1}+(T_{1,\mathrm{II}}{}^H)^{-1}, \quad (2)$$

where $\tau_N(N=\mathrm{I}$ or II) stands for the correlation times τ_c of ammonium ions of either type I or II, $\omega_1=\gamma H_1$, obs stands for observed, and the correlation times are defined as before.[3] Following the convention[3] for $(NH_4)_2SO_4$, type-II ammonium ions are more mobile than those of type I.

[11] D. E. O'Reilly and T. Tsang, J. Chem. Phys. **46**, 1291 (1967); Sec. IV, Eqs. (11), (14), (16), and (17).

The fluorine spin-lattice relaxation time T_1^F is determined mainly by the random modulation of the H-F dipole–dipole interactions due to ammonium-ion reorientations. The H-F interactions are much weaker than H-H interactions because of longer interatomic distances, hence T_1^F is much longer than T_1^H. The time T_1^F can be calculated by the same method previously used[12] for methylammonium ions. Let the subscripts I, i and S, k be used for F and H respectively, then[5c]:

$$(T_1^F)^{-1}=\gamma_I{}^2\gamma_S{}^2\hbar^2S(S+1)$$
$$\times\sum_k\tfrac{1}{12}[J_{ik}{}^{(0)}(\omega_I-\omega_S)+18J_{ik}{}^{(1)}(\omega_I)+9J_{ik}{}^{(2)}(\omega_I+\omega_S)]. \quad (3)$$

In Eq. (3), Abragam's notations[5c] are used. Suppose there is only one type of ammonium ion, with four possible proton positions $k=1$, 2, 3, 4. On neglecting time-independent terms, one finds[3]

$$\sum_k\langle F_{ik}{}^{(q)}(t)F_{ik}{}^{(q)*}(t+\tau)\rangle=[\exp(-\tau/\tau_c)]$$
$$\times[3\sum_k|F_{ik}{}^{(q)}|^2-\sum_{k,j}{}'F_{ik}{}^{(q)*}F_{ij}{}^{(q)}]/4, \quad (4)$$

where the prime on the sum over k and j indicates that $k\neq j$. The autocorrelation function of Eq. (4) may be evaluated if the detailed structure of the substance is known. Unfortunately the detailed structure of $(NH_4)_2BeF_4$ is not known and we shall be required to find an approximate expression for Eq. (4). In the limiting case that one proton is much closer to the fluorine than any of the others, the second summation inside the brackets may be dropped. In the limit that all the protons are far from the fluorine (and thus effectively at the same position) the two sums cancel each other, and the result is zero. Our approximation consists in replacing Eq. (4) by the average of these

[12] D. E. O'Reilly and T. Tsang, Phys. Rev. **157**, 417 (1967).

two limiting cases. Equation (4) then becomes as follows:

$$\sum_k \langle F_{ik}^{(q)}(t) F_{ik}^{(q)*}(t+\tau)\rangle = \tfrac{3}{8}\exp(-\tau/\tau_c)\sum_k |F_{ik}^{(q)}|^2. \quad (5)$$

For powder samples, the spatial averages of $|F_{ik}^{(q)}|^2$ may be used; therefore

$$\langle F_{ik}^{(0)}(t) F_{ik}^{*(0)}(t+\tau)\rangle = \tfrac{3}{10}[\exp(-\tau/\tau_c)]\sum_k r_{ik}^{-6},$$

$$\langle F_{ik}^{(1)}(t) F_{ik}^{*(1)}(t+\tau)\rangle = \tfrac{1}{20}[\exp(-\tau/\tau_c)]\sum_k r_{ik}^{-6},$$

$$\langle F_{ik}^{(2)}(t) F_{ik}^{*(2)}(t+\tau)\rangle = \tfrac{1}{5}[\exp(-\tau/\tau_c)]\sum_k r_{ik}^{-6}.$$

The sum $\sum_k r_{ik}^{-6}$ can be related to M_2^{F}, the contribution to fluorine second moment due to H-F dipole-dipole interactions. For powders,[5b] $M_2^{\mathrm{F}} = \frac{1}{5}(\gamma_{\mathrm{H}}^2\hbar^2\sum_k r_{ik}^{-6})$, where the sum is over all neighboring protons. Taking the Fourier transform and including all neighboring tetrahedra, we get

$$\frac{1}{T_1^{\mathrm{F}}} = \frac{3}{16}\gamma_{\mathrm{F}}^2 M_2^{\mathrm{F}}\left[\frac{\tau_c}{1+\omega'^2\tau_c^2} + \frac{3\tau_c}{1+\omega^2\tau_c^2} + \frac{6\tau_c}{1+4\omega^2\tau_c^2}\right], \quad (6)$$

where $\omega' = |\omega_I - \omega_S| = 0.063\omega$, and $\omega_I + \omega_S$ was approximated by 2ω. In $(NH_4)_2BeF_4$, we have two types of ammonium ions. Assuming each type contributes half of the second moment, then:

$$\frac{1}{T_1^{\mathrm{F}}} = \frac{3}{32}\gamma_{\mathrm{F}}^2 M_2^{\mathrm{F}}\left[\frac{\tau_{\mathrm{I}}}{1+\omega'^2\tau_{\mathrm{I}}^2} + \frac{3\tau_{\mathrm{I}}}{1+\omega^2\tau_{\mathrm{I}}^2} + \frac{6\tau_{\mathrm{I}}}{1+4\omega^2\tau_{\mathrm{I}}^2} + \frac{\tau_{\mathrm{II}}}{1+\omega'^2\tau_{\mathrm{II}}^2} + \frac{3\tau_{\mathrm{II}}}{1+\omega^2\tau_{\mathrm{II}}^2} + \frac{6\tau_{\mathrm{II}}}{1+4\omega^2\tau_{\mathrm{II}}^2}\right]. \quad (7)$$

For spin-lattice relaxation due to dipolar interactions between unlike spins I and S (for F^{19} and protons, respectively), it is well known[5c] that the spins are coupled:

$$d\langle I_z\rangle/dt = -(T_1^{II})^{-1}\langle I_z - I_0\rangle - (T_1^{IS})^{-1}\langle S_z - S_0\rangle$$

$$d\langle S_z\rangle/dt = -(T_1^{SI})^{-1}\langle I_z - I_0\rangle - (T_1^{SS})^{-1}\langle S_z - S_0\rangle, \quad (8)$$

where $\langle I_z\rangle$ and $\langle S_z\rangle$ are the thermal average values of the z component magnetizations; I_0 and S_0 are the equilibrium values of $\langle I_z\rangle$ and $\langle S_z\rangle$. In Appendix A, it is shown that the observed T_1^{-1} values are the eigenvalues of the matrix:

$$\begin{pmatrix} (T_1^{II})^{-1} & (T_1^{IS})^{-1} \\ (T_1^{SI})^{-1} & (T_1^{SS})^{-1} \end{pmatrix}. \quad (8')$$

T_1^{II}, T_1^{SI} and T_1^{IS} are related to H-F dipolar interactions, and are of comparable magnitude. On the other hand, T_1^{SS} is much shorter. It can readily be shown that the F^{19} and H^1 spin-lattice relaxations are very close to being exponential, with observed values of T_1 very close to T_1^{II} and T_1^{SS} themselves; and it is not necessary to evaluate T_1^{SI} and T_1^{IS}. On the other hand, at higher temperatures ($10^3/T<4$), the relative magnitudes of all the above matrix elements are comparable to each other; and nonexponential behavior is expected. The details are given in Sec. B.

M_2^{F} is the F^{19} second moment due to the dipolar interaction between fixed BeF_4 and fixed NH_4 ions. Unfortunately, the proton positions in $(NH_4)_2BeF_4$ have not been determined. If we assume that $(NH_4)_2BeF_4$ and $(NH_4)_2SO_4$ are isomorphic, then $M_2 = 7$ G^2 from Schlemper and Hamilton's structure[13] for $(NH_4)_2SO_4$. For $4.5<10^3/T<6.5$, both $\omega\tau_{\mathrm{I}} \ll 1$ and $\omega\tau_{\mathrm{II}} \ll 1$; Eqs. (1), (2), and (7) can be written as

$$T_{1,\mathrm{obs}}^{\mathrm{H}} = 3.1\times10^{-11}/(\tau_{\mathrm{I}}+\tau_{\mathrm{II}})$$

and

$$T_1^{\mathrm{F}} = 2.4\times10^{-10}/(\tau_{\mathrm{I}}+\tau_{\mathrm{II}}),$$

which gives $T_1^{\mathrm{F}} = 8T_{1,\mathrm{obs}}^{\mathrm{H}}$ in reasonable agreement with experimental results in Fig. 1.

For $4<10^3/T<7$, the reorientation of type-I ammonium ions is the dominating proton spin-lattice relaxation mechanism, and τ_{I} is calculated directly from T_1^{H} data using Eqs. (1) and (2). Similarly, τ_{I} can be calculated directly from $T_{1\rho}^{\mathrm{H}}$ data for $7<10^3/T<9$ (see Sec. IIIC), and τ_{II} from T_1^{H} data for $10^3/T>11$. The results are summarized in Fig. 3.

From τ_{I} and τ_{II} given in Fig. 3, we have calculated T_1^{F} from Eq. (7), and also T_1^{H} for $7<10^3/T<10$,

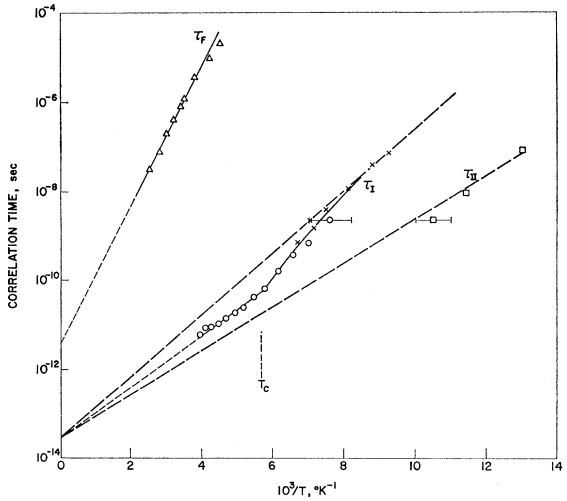

FIG. 3. Correlation times of NH_4 (τ_{I}, τ_{II}) and BeF_4 (τ_{F}) ions versus inverse temperature on semilogarithm scale. (For τ_{I}, the circles and crosses are correlation times derived from proton T_1 and $T_{1\rho}$ measurements, respectively, and the solid line is drawn assuming that the potential-barrier height is a linear function of the square of spontaneous polarization.)

[13] E. O. Schlemper and W. C. Hamilton, J. Chem. Phys. **44**, 4498 (1966).

where both types I and II ammonium-ion reorientations contribute to proton relaxation. The calculated results are given in Fig. 1, and agree well with experimental data. Evidently the averaging approximation made in the simplification of Eq. (4) is a reasonable estimate.

B. T_1 Data at High Temperatures

For $T>250°$K, a new relaxation mechanism for the protons and F^{19} nuclei becomes important. This mechanism (denoted by the subscript HF) is associated with the modulation of the H–F dipolar interactions by the reorientation of the BeF_4^{2-} groups, the correlation time of which will be denoted as τ_F. As shown in Appendix B, Eq. (3) may also be expressed in terms of the quantity M_2^F:

$$(T_1^F)_{HF}^{-1}=\tfrac{3}{32}\gamma_F^2 M_2^F \times\left[\frac{\tau_F}{1+\omega'^2\tau_F^2}+\frac{3\tau_F}{1+\omega^2\tau_F^2}+\frac{6\tau_F}{1+4\omega^2\tau_F^2}\right]. \quad (9)$$

By reference to Fig. 1, it may be seen that the relaxation produced by the reorientation of the NH_4^+ tetrahedra is quite negligible above 250°K, and only the contribution of the relatively slow reorientation of the BeF_4^{2-} groups has been included in Eq. (9). Since there are twice as many protons as fluorine nuclei, $(T_1^H)_{HF}^{-1}=\frac{1}{2}(T_1^F)_{HF}^{-1}$. In a similar manner we may calculate the off-diagonal relaxation times T_1^{HF} and T_1^{FH}. As derived by Abragam,[5c]

$$(T_1^{FH})^{-1}=2(T_1^{HF})^{-1} =(\gamma_F^2\gamma_H^2\hbar^2/16)\sum_j\{-J_{ij}^{(0)}(\omega')+9J_{ij}^{(2)}(2\omega)\}. \quad (10)$$

$(T_1^{FH})^{-1}$ is twice as large as $(T_1^{HF})^{-1}$ since there are twice as many protons as fluorine nuclei. By the method of Appendix B, Eq. (10) may also be written in terms of M_2^F:

$$(T_1^{FH})^{-1}=2(T_1^{HF})^{-1} =\tfrac{3}{32}\gamma_F^2 M_2^F\left\{-\frac{\tau_F}{1+\omega'^2\tau_F^2}+\frac{6\tau_F}{1+4\omega^2\tau_F^2}\right\}. \quad (11)$$

As before, we have approximated $\omega_F+\omega_H$ by 2ω.

In addition, the F-F and Be-F dipolar interactions contribute to T_1^F; and these contributions may be calculated by methods[3] used for $(NH_4)_2SO_4$. Using 1.61 Å for the Be-F distance, we obtain

$$(T_1^F)_F^{-1}=1.6\times10^9\left\{\frac{\tau_F}{1+\omega^2\tau_F^2}+\frac{4\tau_F}{1+4\omega^2\tau_F^2}\right\}, \quad (12a)$$

$$(T_1^F)_{Be}^{-1}=3.0\times10^9\left\{\frac{\tau_F}{1+\omega^2\tau_F^2}\right\}. \quad (12b)$$

Coupling of the fluorine spin system with the beryllium spin system is relatively weak in the temperature range under consideration, because $\omega_F-\omega_{Be}$ is not small compared to ω_F (whereas, $|\omega_F-\omega_H|\ll\omega_F$); and the off-diagonal elements $(T_1^{BeF})^{-1}$ and (T_1^{FBe}) do not become large as does $(T_1^{FH})^{-1}$ and $(T_1^{HF})^{-1}$. In Eq. (12b), $\omega_F+\omega_{Be}$ and $\omega_F-\omega_{Be}$ have been approximated by $\omega_F=\omega$. Combining Eqs. (9) and (12), and including the effect of NH_4^+ ion reorientation in T_1^{HH}, we obtain

$$(T_1^{FH})^{-1}=2(T_1^{HF})^{-1} =-\alpha+\tfrac{9}{32}\gamma_F^2 M_2^F\left(\frac{\tau_F}{1+\omega^2\tau_F^2}+\frac{4\tau_F}{1+4\omega^2\tau_F^2}\right) =-\alpha+\alpha\epsilon_2, \quad (13)$$

$$(T_1^{HH})^{-1}=(\alpha/2)+(3.2\times10^{10})(\tau_I+\tau_{II}) =(\alpha/2)+\alpha\epsilon_3, \quad (14)$$

$$(T_1^{FF})^{-1}=\alpha+(1.6\times10^9)\left(\frac{\tau_F}{1+\omega^2\tau_F^2}+\frac{4\tau_F}{1+4\omega^2\tau_F^2}\right) +(3.0\times10^9)\left(\frac{\tau_F}{1+\omega^2\tau_F^2}\right) =\alpha+\alpha\epsilon_1 \quad (15)$$

$$\alpha=\tfrac{3}{32}\gamma_F^2 M_2^F\left(\frac{\tau_F}{1+\omega'^2\tau_F^2}+\frac{3\tau_F}{1+\omega^2\tau_F^2}+\frac{6\tau_F}{1+4\omega^2\tau_F^2}\right),$$

where ϵ_1, ϵ_2, and ϵ_3 are defined as above.

The observed spin-lattice relaxation times are obtained by diagonalizing the relaxation matrix (8a), using matrix elements given by Eqs. (13) through (15).

From the second-moment transition[10] near −60°C, τ_F is estimated[5d] to be approximately 10^{-5} sec at that temperature; and both $\omega\tau_F$ and $\omega'\tau_F$ are much larger than unity. We therefore expect the ω' terms to be the dominating terms. This means that the matrix elements of the relaxation matrix are either α or $\frac{1}{2}\alpha$ plus small correction terms in $\epsilon_i\alpha$, ϵ_i being much less than unity. On diagonalization of the relaxation matrix, the observed spin-relaxation times T_1' and T_1'' ($T_1'\ll T_1''$) are given by the following two eigenvalues:

$$(T_1')^{-1}=\tfrac{3}{2}\alpha, \quad (16)$$

$$(T_1'')^{-1}=\tfrac{1}{3}\alpha(\epsilon_1+2\epsilon_2+2\epsilon_3). \quad (17)$$

In the measurement of fluorine spin-lattice relaxation times with the 180°–90° pulse sequence, an initial magnetization $\langle I_z\rangle=-I_0$ is created at $t=0$. Neglecting terms of the order of ϵ, the solution of Eq. (8) is as follows (see Appendix A):

$$[I_0-\langle I_z\rangle]/I_0=\tfrac{4}{3}\exp(-t/T_1')+\tfrac{2}{3}\exp(-t/T_1''). \quad (18)$$

Similarly, the proton spin-lattice relaxation is given by

$$[S_0-\langle S_z\rangle]/S_0=\tfrac{2}{3}\exp(-t/T_1')+\tfrac{4}{3}\exp(-t/T_1''). \quad (19)$$

For both F^{19} and H^1, the recovery of the nuclear magnetization contains two components of comparable

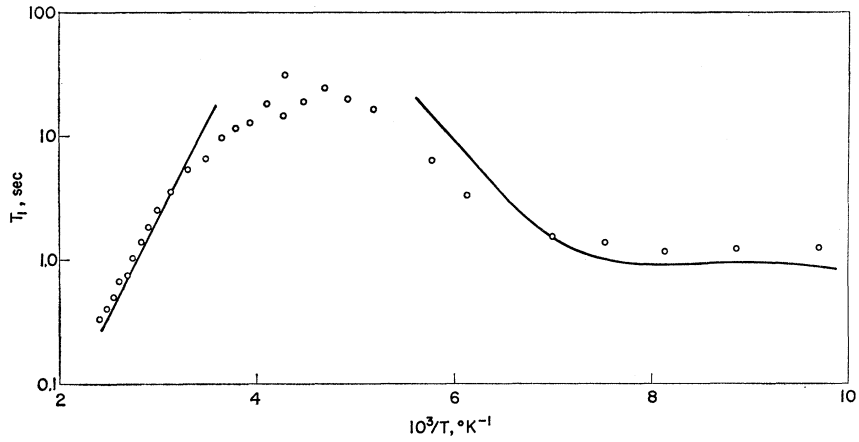

FIG. 4. T_1 data for F^{19} in polycrystalline $(ND_4)_2BeF_4$ at 42 Mc/sec versus inverse temperature (semilogarithmic scale). The curve is calculated from correlation times given in Fig. 3.

intensity, but quite different time constants. A typical experimental result is shown in Fig. 2, along with the results calculated from Eqs. (13) to (19) with values of τ_F obtained as described below.

When $\omega'\tau_F \gg 1$, but $10^3/T > 3.5$, $\alpha = 1.5\times10^{-6}/\tau_F$, $\epsilon_1 = 0.059$, $\epsilon_2 = 0.024$, $\epsilon_3 \leq 0.10$, and $T_1' = 4.4\times10^5\ \tau_F$; hence, $T_1'' = \frac{9}{2}\ T_1'/(\epsilon_1+2\epsilon_2+2\epsilon_3) \geq 15\ T_1'$. At $10^3/T = 3$, $T_1'' \approx 25\ T_1'$ from Fig. 1 in reasonable agreement with the calculated value. From Eq. (15) it may be seen that T_1' attains a minimum value of 0.06 sec when $\omega'\tau_F = 1$ or $\tau_F = 6.0\times10^{-8}$ sec. The experimental minimum value of T_1' from Fig. 1 is 0.08 ± 0.02 sec.

Values of τ_F were calculated from the T_1' data of Fig. 1 and then values of T_1'' were calculated from the values of τ_F. Calculated curves of T_1' and T_1'' are given in Fig. 1, and the corresponding values of τ_F are given in Fig. 3. The calculated curves fit the data well. The τ_F values are also consistent with the reduction in fluorine second moment near -50°C, as observed by Burns,[10] for which we calculate $\tau_F = 2\times10^{-5}$ sec.

C. $T_{1\rho}$ Data for $(NH_4)_2BeF_4$

We will now show that the NH_4- and BeF_4-ion correlation times are consistent with $T_{1\rho}$ data given in Fig. 1. $T_{1\rho}$ for dipolar relaxation between both like and unlike spins has been derived in Appendix C.

A maximum in $T_{1\rho}^H$ was observed (see Fig. 1) near $10^3/T = 6$. At lower temperatures, $T_{1\rho}^H$ is determined by the reorientation of NH_4 tetrahedra and can be readily calculated.[3] In Fig. 1, we have shown the calculated $T_{1\rho}^H$ values using τ_I and τ_{II} given in Fig. 3. The agreement with experimental data is good.

In the high-temperature range ($10^3/T < 6$), $T_{1\rho}^H$ is determined by the reorientation of BeF_4 tetrahedra and the dipolar interaction between H and F nuclei. Using T_2 given by Abragam[5c] for unlike spins, we get (see Appendix C)

$$(T_{1\rho}^H)^{-1} = \gamma_I^2\gamma_S^2\hbar^2 S(S+1) \times[4J^{(0)}(\omega_1)+J^{(0)}(\omega')+54J^{(1)}(\omega)+9J^{(2)}(2\omega)]/24.$$

Relating the J's to the second moment M_2^F as discussed in Sec. A, we get

$$(T_{1\rho}^H)^{-1} = \frac{3\gamma_F^2 M_2^F}{64}\left[\frac{4\tau_F}{1+\omega_1^2\tau_F^2}+\frac{\tau_F}{1+\omega'^2\tau_F^2} + \frac{9\tau_F}{1+\omega^2\tau_F^2}+\frac{6\tau_F}{1+4\omega^2\tau_F^2}\right]. \quad (20)$$

Choosing $M_2^F = 7$ G^2 as in Sec. IIIB, we get the minima $T_{1\rho}^H = 1\times10^{-3}$ sec at $\tau_c = 2.5\times10^{-6}$ sec for the experimental $H_1 = 16$ G, in good agreement with the experimental minima 9×10^{-4} sec. From τ_F given in Fig. 3, we have calculated and plotted $T_{1\rho}^H$ versus $10^3/T$ in Fig. 1. The calculated curve follows the general behavior of the observed values, but the experimental values are noticeably shorter at intermediate temperatures.

D. F^{19} T_1 Data in $(ND_4)_2BeF_4$

To verify the mechanism proposed for the nonexponential relaxation discussed in Sec. IIIB, T_1 for F^{19} in polycrystalline $(ND_4)_2BeF_4$ has also been measured. The results are summarized in Fig. 4. The relaxation is exponential and for $10^3/T < 4$, T_1 is not greatly different from T_1'' in Fig. 1. In Sec. IIIB, it is postulated that the nonexponential behavior of spin-lattice relaxation in $(NH_4)_2BeF_4$ is due to the presence of two types of dipole–dipole interactions: the H-F interaction is related to the shorter component with characteristic time T_1', and the F-F and Be-F interactions are related to the longer component T_1''. The T_1 data for $(ND_4)_2BeF_4$ give further evidence for this mechanism, the substitution of deuterons for protons being the cause of the disappearance of the T_1' component.

In Fig. 4, values of T_1 calculated from correlation times given in Fig. 3 are also shown. For $10^3/T < 4$, T_1^{-1} is calculated by adding (12a) and (12b) since we expect the main F^{19} spin-lattice relaxation mechanism to be via the F-F and Be-F dipolar interactions; whereas, the contribution from the D-F interaction

is quite negligible since there is no longer any term involving a small ω'. For $10^3/T>4$, it was shown in Sec. IIIA that F^{19} spin-lattice relaxation is mainly due to reorientation of NH_4^+ tetrahedra. The D-F dipolar interaction is a factor of 16 weaker than H-F interaction. τ_I and τ_{II} for $(ND_4)_2BeF_4$ are also expected to be a factor of $\sqrt{2}$ longer than that for $(NH_4)_2BeF_4$, based on the classical rotator approximation.[3] T_1^F is obtained from Eq. (7) with $\omega'=\omega_F-\omega_D\approx\omega_F+\omega_D\approx\omega$.

$$(T_1^F)^{-1}=\tfrac{1}{16}\tfrac{5}{16}\gamma_F^2 M_2^F\left(\frac{\tau_I}{1+\omega^2\tau_I^2}+\frac{\tau_{II}}{1+\omega^2\tau_{II}^2}\right), \quad (21)$$

where M_2^F is $\frac{1}{16}$ as large as the fluorine second moment used in Sec. IIIA, and τ_I and τ_{II} are $\sqrt{2}$ times as long as the values in Fig. 3. The solid curve on the right side of Fig. 4 is calculated from Eq. (21).

The over-all agreement between calculation and experiment is good except for the region $T_1^F(\text{calc})>30$ sec. In this region, the relaxation can be dominated by other mechanisms, such as the presence of traces of paramagnetic impurities.

IV. DEUTERON RESONANCE RESULTS

Over the experimental temperature range (77 to 300°K), only motionally averaged deuteron resonance lines were observed, with separations of 15 G or less. Measurements have been made at −85° (paraelectric), −110 and −150°C (ferroelectric). There was no abrupt temperature dependence of the rotation patterns. Two sets of deuteron quadrupolar coupling tensors were observed, one of them very close to zero; the other one is tabulated as follows in kc/sec (uncertainty about ±0.5):

	V_{aa}	V_{bb}	V_{cc}	$\lvert V_{ab}\rvert$	$\lvert V_{bc}\rvert$	$\lvert V_{ca}\rvert$
−85°	±3.5	∓3.5	0	2.0	0	0
−110°	±3.9	∓3.0	∓0.9	3.0	0	0
−150°	±4.3	∓4.3	0	3.6	0	0
$(ND_4)_2SO_4$ Type II	±4.2	∓5.7	±1.5	2.6	0	2.3

The tensor components for $(ND_4)_2SO_4$ are the values[3] for type-II ND_4 ions at −60°C. The net dipole moments for the two types of ammonium ions in $(ND_4)_2BeF_4$ are estimated[3] to be 0 and 0.09 D; the average of these values is somewhat smaller than the value 0.11 D calculated for either type I or II ammonium ion[3] in $(ND_4)_2SO_4$. The x principal axis is perpendicular to the ab plane and within experimental uncertainties ($\sim\pm10°$ in orientation) the principal coordinate system does not alter in orientation with temperature. This is in contrast to the abrupt reorientation of the principal coordinate systems observed in $(ND_4)_2SO_4$ at the Curie point.[3]

It should be noted that in the calculation of the distortion of the NH_4^+ ion from the observed quadrupolar coupling tensor contributions to the field gradient at a deuteron due to the remainder of the lattice are not included. These contributions may, in principle, be comparable due to the distortion of the NH_4^+ ion from tetrahedral symmetry, but are difficult to calculate due to the hydrogen bonds that are present.

TABLE I. Activation energies (ΔE, kcal/mole) and pre-exponential factors (τ_c^0, sec) for $(NH_4)_2BeF_4$.

Ion and temperature range	ΔE	τ_c^0
BeF_4^{2-}: $T>T_c$	7.3	3×10^{-12}
NH_4^+, I: $T>T_c$	2.7	3×10^{-14}
$T<110$°K	3.3	3×10^{-14}
NH_4^+, II: $T<110$°K	2.3	3×10^{-14} (estimated)

V. MOLECULAR MOTION AND FERROELECTRICITY

The deuteron resonance results in Sec. IV indicate that the average dipole moment per ammonium ion in $(ND_4)_2BeF_4$ is about half of that in $(ND_4)_2SO_4$. The observed spontaneous polarization of $(NH_4)_2BeF_4$ at low temperature is about half of that for $(NH_4)_2SO_4$. This is in agreement with the results of recent magnetic resonance studies on ammonium sulfate[3] and ammonium alums,[12] which indicate that the ferroelectricity in these substances arises from the distortion of the ammonium ions.

Above T_c and below 130°K the correlation time data of Fig. 3 may be represented by $\tau_c=\tau_c^0\exp(\Delta E/RT)$; the activation energies ΔE and pre-exponential factors τ_c^0 are given in Table I. The pre-exponential factors are in order of magnitude agreement with those calculated from the classical rotator model[3] ($\tau_c^0=6\times10^{-14}$ and 4×10^{-13} sec for NH_4^+ and BeF_4^{2-}, respectively). In a temperature range of about 35° below T_c the correlation time for type I NH_4^+ ion deviates significantly from the straight lines at higher and lower temperatures in Fig. 3. This effect is similar to that observed[3] for $(NH_4)_2SO_4$ for which ΔE depends linearly on the anomalous volume contraction of the crystal. This was interpreted[14] as a dependence of ΔE on the number of misoriented pairs of ions below T_c, or equivalently, in the molecular field approximation, as a dependence of ΔE on the square of the spontaneous polarization. With this assumption, τ_I was calculated from the experimental spontaneous polarization data[1] and is plotted in Fig. 3.

The ferroelectric properties of $(NH_4)_2BeF_4$ have been studied by various workers.[1,15,16] The transition is

[14] D. E. O'Reilly and T. Tsang, J. Chem. Phys. **46**, 1301 (1967).
[15] H. Ohshima and E. Nakamura, J. Phys. Chem. Solids **27**, 481 (1966).
[16] B. A. Strukov, N. D. Gavrilyuk, and V. A. Koptsik, Kristallografiya **6**, 780 (1961) [English transl.: Soviet Phys.—Cryst. **6**, 625 (1961)].

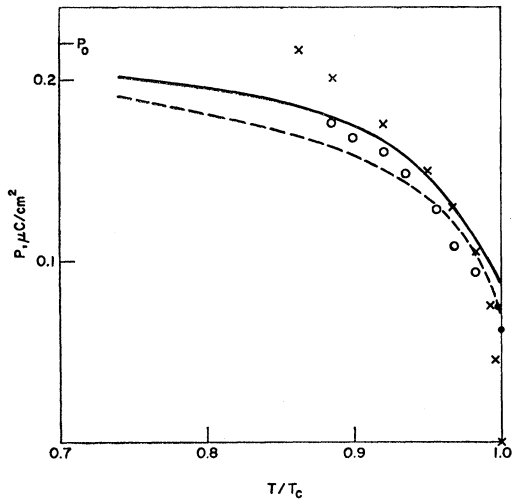

FIG. 5. Spontaneous polarization P, $\mu C/cm^2$, versus reduced temperature T/T_c. Experimental data: circles—Strukov, Gavrilyuk, and Koptsik (Ref. 15); crosses—Hoshino, Vedam, Okaya, and Pepinsky (Ref. 1). Solid line, calculated by minimizing (22), $P_0=0.22$; dashed line, calculated from the Strukov and Koptsik (Ref. 17) parameters using Devonshire's theory.

gradual; and, although it is first order, it is very close to being a second-order transition in contrast to the transition in $(NH_4)_2SO_4$, which is quite abrupt. The transition in $(NH_4)_2SO_4$ may be described by a modified molecular field approximation.[14] In this model, a dipole is restricted to a point along one of two directions with probabilities n_+ and n_-. The free energy $\Delta F(x)$, which depends on $x=n_+-n_-$, may be written as follows (per molecule):

$$\Delta F(x)=-\tfrac{1}{2}(Ax^2)-\tfrac{1}{4}(Bx^4)+\tfrac{1}{2}kT \times[(1+x)\ln(1+x)+(1-x)\ln(1-x)]. \quad (22)$$

It may be shown[14] that if $b=B/A>\frac{1}{3}$, the transition is first order; while, if $b<\frac{1}{3}$, it is second order. For $(NH_4)_2SO_4$, $b=0.5$. The parameter b may be calculated from the experimental values of T_0 and T_c, where T_0 is the Curie–Weiss constant. For $(NH_4)_2BeF_4$,[17] $(T_c-T_0)/T_c\approx 1.7\times 10^{-3}$ and $b-\frac{1}{3}=0.044$. The spontaneous polarization $P=xP_0$ is plotted as the solid line in Fig. 5, where P_0 is the spontaneous polarization at 0°K which is taken to be 0.22 $\mu C/cm^2$. The agreement with the experimental data of Hoshino *et al.*[1] and Strukov *et al.*[16] is satisfactory. Strukov and Koptsik[17] have applied the Devonshire phenomenological theory[18] to $(NH_4)_2SO_4$. The calculated spontaneous polarization (dashed curve in Fig. 5) also agrees fairly well with the experimental data.

In analogy to $(NH_4)_2SO_4$ one may expect that the transition in $(NH_4)_2BeF_4$ is due to a tilting of the NH_4^+ ions either parallel or antiparallel to the ferroelectric axis. However, in $(NH_4)_2BeF_4$ this axis is the crystal b axis in contrast to $(NH_4)_2SO_4$ where the ferroelectric axis is the c axis. Such tilting of the NH_4^+ may be explained by the presence of a double minimum potential energy surface with one minimum above a plane perpendicular to the ferroelectric axis, and the other equally displaced below this plane. As shown by the studies of Hoshino *et al.*,[1] on the system $(NH_4)_2(BeF_4)_{1-x}(SO_4)_x$, for $0.7\gtrsim x\gtrsim 0.2$ the system shows no ferroelectric transition in the temperature range −196°C to 25°C. Thus the double minimum potential appears to be a very sensitive function of the composition of the system and shifts from along the c-axis direction to along the b-axis direction as x changes from zero to one. Unfortunately no detailed neutron diffraction study has been made on $(NH_4)_2BeF_4$, and little can be said concerning the detailed mechanism of the ferroelectric transition.

APPENDIX A: SOLUTION OF THE COUPLED SPIN-LATTICE RELAXATION EQUATIONS

Equations (8) may be conveniently solved by the Laplace-transform method.[19] Let us define $\mathcal{I}=\langle I_z-I_0\rangle$ and $\mathcal{S}=\langle S_z-S_0\rangle$. The Laplace transform of Eq. (8) may be written as follows:

$$-\mathcal{I}(0)+s\mathfrak{I}=-(T_1^{II})^{-1}\mathfrak{I}-(T_1^{IS})^{-1}\mathfrak{S}'$$
$$-\mathcal{S}(0)+s\mathfrak{S}=-(T_1^{SI})^{-1}\mathfrak{I}-(T_1^{SS})^{-1}\mathfrak{S}, \quad (A1)$$

where

$$\mathfrak{I}(s)=\int_0^\infty e^{-st}\mathcal{I}(t)\,dt,$$

and $\mathfrak{S}$ are the Laplace transforms of $\mathcal{I}$ and $\mathcal{S}$, respectively, and $\mathcal{I}(0)$ is the value of $\mathcal{I}$ at $t=0$. Equations (A1) may be solved for $\mathfrak{I}$ and $\mathfrak{S}$; the initial conditions of interest are $\mathcal{I}(0)=-2I_0$ or $\mathcal{S}(0)=-2S_0$. One obtains

$$\mathfrak{I}=\frac{2I_0\{(T_1^{SS})^{-1}+s\}}{\{-(T_1^{SS})^{-1}-s\}\{(T_1^{II})^{-1}-s\}-(T_1^{IS})^{-1}(T_1^{SI})^{-1}} \quad (A2)$$

and a similar expression for $\mathfrak{S}$. The inverse transform of $\mathfrak{I}$ is now taken to yield

$$\mathcal{I}=(2\pi i)^{-1}\int_{-i\infty}^{i\infty}\frac{2I_0\{(T_1^{SS})^{-1}+s\}e^{st}}{(s-s_1)(s-s_2)}\,ds, \quad (A3)$$

where $-s_1$ and $-s_2$ are the eigenvalues of the relaxation matrix (8a), and the integration extends along the imaginary axis and over an infinite semicircle around

[17] B. A. Strukov and V. A. Koptsik, Kristallografiya **7**, 234 (1962) [English transl.: Soviet Phys.—Cryst. **7**, 182 (1962)].
[18] A. F. Devonshire, Advan. Phys. **3**, 85 (1954).
[19] See, for example, R. V. Churchill, *Modern Operational Mathematics in Engineering* (McGraw-Hill Book Company, Inc., New York, 1944), pp. 2, 6, 44, and 157.

the left half-plane. Performing the integrations we obtain

$$\mathcal{G}=2I_0\left\{\frac{((T_1^{SS})^{-1}+s_1)e^{s_1t}}{s_1-s_2}+\frac{((T_1^{SS})^{-1}+s_2)e^{s_2t}}{s_2-s_1}\right\}, \quad \text{(A4)}$$

$$\mathcal{S}=2S_0\left\{\frac{((T_1^{II})^{-1}+s_1)e^{s_1t}}{s_1-s_2}+\frac{((T_1^{II})^{-1}+s_2)e^{s_2t}}{s_2-s_1}\right\}. \quad \text{(A5)}$$

Placing the values of parameters into Eqs. (A4) and (A5), the solutions given in Eqs. (18) and (19) are obtained.

APPENDIX B: AUTOCORRELATION FUNCTION FOR ROTATING TETRAHEDRA

Let us consider the autocorrelation function of $F_{ij}^{(q)}$ for the case that both the NH_4^+ and BeF_4^{2-} groups are rotating. Consider first a pair of tetrahedra and denote the correlation times for tetrahedral reorientation by τ_H and τ_F, then by the same method of derivation of Eq. (4)[3] we have

$$\begin{aligned}F_{ij}(t+\tau)=&[\tfrac{1}{4}+\tfrac{3}{4}\exp(-\tau/\tau_H)][\tfrac{1}{4}+\tfrac{3}{4}\exp(-\tau/\tau_F)]F_{ij}\\&+\sum_{k\neq j}F_{ik}[\tfrac{1}{4}-\tfrac{1}{4}\exp(-\tau/\tau_H)][\tfrac{1}{4}+\tfrac{3}{4}\exp(-\tau/\tau_F)]\\&+\sum_{l\neq i}F_{lj}[\tfrac{1}{4}+\tfrac{3}{4}\exp(-\tau/\tau_H)][\tfrac{1}{4}-\tfrac{1}{4}\exp(-\tau/\tau_F)]\\&+\sum_{k\neq j,\,l\neq i}F_{lk}[\tfrac{1}{4}-\tfrac{1}{4}\exp(-\tau/\tau_H)][\tfrac{1}{4}-\tfrac{1}{4}\exp(-\tau/\tau_F)],\end{aligned} \quad \text{(B1)}$$

where the superscript q has been omitted for simplicity. Retaining only terms in $\exp(-\tau/\tau_F)$ since $\tau_H\ll\tau_F$,

$$\begin{aligned}\langle F_{ij}(t)F_{ij}^*(t+\tau)\rangle=&\exp(-\tau/\tau_F)\\&\times\{\tfrac{3}{16}|F_{ij}|^2+\tfrac{3}{16}\sum_{k\neq j}F_{ik}^*F_{ij}\\&-\tfrac{1}{16}\sum_{l\neq i}F_{lj}^*F_{ij}-\tfrac{1}{16}\sum_{k\neq j,\,l\neq i}F_{lk}^*F_{ij},\},\end{aligned} \quad \text{(B2)}$$

and further

$$\begin{aligned}\tfrac{1}{4}\sum_{ij}\langle F_{ij}(t)F_{ij}^*(t+\tau)\rangle=&\tfrac{1}{4}\exp(-\tau/\tau_F)\\&\times\{3\sum_i\bar{F}_i\bar{F}_i^*-\sum_{l\neq i}\bar{F}_l\bar{F}_i^*\},\end{aligned} \quad \text{(B3)}$$

where $\bar{F}_i=\frac{1}{4}\sum_jF_{ij}$ is an average value of F_{ij} for the ith fluorine nucleus. The indices i, l refer to fluorine nuclei and k, j refer to protons. As with the sums occurring in Eq. (4), the sums which appear in Eq. (B3) depend on the detailed structure of $(NH_4)_2BeF_4$. For this reason we shall approximate Eq. (B3) as follows:

$$\tfrac{1}{4}\sum_{ij}\langle F_{ij}(t)F_{ij}(t+\tau)\rangle\approx\tfrac{3}{4}\exp(-\tau/\tau_F)\bar{F}_{i'}\bar{F}_{i'}^*, \quad \text{(B4)}$$

where i' is the fluorine nucleus closest to the neighboring NH_4^+ tetrahedron. The product $\bar{F}_{i'}\bar{F}_{i'}^*$ averaged over a sphere may be approximated as follows:

$$\begin{aligned}&\tfrac{1}{4}\sum_{ij}\langle F_{ij}^{(0)}(t)F_{ij}^{(0)*}(t+\tau)\rangle\\&\qquad=(\tfrac{3}{64})(\tfrac{4}{5})\exp(-\tau/\tau_F)(\sum_j r_{i'j}^{-6}),\\&\tfrac{1}{4}\sum_{ij}\langle F_{ij}^{(1)}(t)F_{ij}^{(1)*}(t+\tau)\rangle\\&\qquad=(\tfrac{3}{64})(\tfrac{2}{15})\exp(-\tau/\tau_F)(\sum_j r_{i'j}^{-6}),\\&\tfrac{1}{4}\sum_{ij}\langle F_{ij}^{(2)}(t)F_{ij}^{(2)*}(t+\tau)\rangle\\&\qquad=(\tfrac{3}{64})(\tfrac{8}{15})\exp(-\tau/\tau_F)(\sum_j r_{i'j}^{-6}).\end{aligned} \quad \text{(B5)}$$

In performing the sum over tetrahedra, it is to be noted that each BeF_4^{2-} is surrounded by 11 nearest-neighbor NH_4^+ groups; but each NH_4^+ is surrounded, on the average, by half this number of BeF_4^{2-} groups, and as a result $(T_1^{IS})^{-1}=2(T_1^{SI})^{-1}$.

APPENDIX C: RELATIONSHIP BETWEEN $T_{1\rho}$ AND T_2

We will first consider relaxation by dipolar–dipolar interactions between two like spins I, $I'=\frac{1}{2}$; and will follow Abragam's notations.[5c,5e] By taking the density matrix trace (denoted by $\langle\ \rangle$) of the operator I_x+I_x', the master equation[5c] may be written as

$$d\langle I_x+I_x'\rangle/dt=-i\langle[\mathcal{H}_0(t)+\mathcal{H}_1(t),\ I_x+I_x']\rangle. \quad \text{(C1)}$$

In the calculation of T_2, the spin Hamiltonian $\mathcal{H}_0$ is set equal to $\omega(I_z+I_z')$ and

$$\begin{aligned}d\langle I_x+I_x'\rangle/dt=&-i\langle[\omega I_z+\omega I_z'+\mathcal{H}_1(t),\ I_x+I_x']\rangle\\=&-\langle I_x+I_x'\rangle/T_2.\end{aligned} \quad \text{(C2)}$$

To solve an equation of the general form $dB/dt=-i[\mathcal{H}_0(t)+\mathcal{H}_1(t),\ B]$, $\mathcal{H}_1$ being the perturbation term, it is convenient to introduce the interaction representation $B^*=UBU^{-1}$ and $\mathcal{H}_1^*=U\mathcal{H}_1U^{-1}$; the function U is chosen to be a solution of $dU/dt=iU\mathcal{H}_0(t)$. In the interaction representation,

$$dB^*/dt=-i[\mathcal{H}_1^*(t),\ B^*]. \quad \text{(C3)}$$

To evaluate T_2 in the interaction representation, $U=\exp(i\omega I_zt+i\omega I_z't)$. By writing $\mathcal{H}_1=\sum_qF^{(q)}A^{(q)}$ with $A^{(q)*}(t)=e^{iq\omega t}A^{(q)}$, Abragam[5c] has shown that

$$T_2^{-1}\langle I_x+I_x'\rangle=\sum_{q=0,\pm1,\pm2}\int_0^\infty\langle F^{(q)}(t)F^{(-q)}(t+\tau)[A^{(q)*}(t),[A^{(-q)*}(t+\tau),\ I_x+I_x']]\rangle d\tau, \quad \text{(C4)}$$

$$T_2^{-1}=\tfrac{9}{32}\gamma^4\hbar^2[J^{(0)}(0)+10J^{(1)}(\omega)+J^{(2)}(2\omega)]. \quad \text{(C5)}$$

The $J^{(0)}$, $J^{(1)}$, and $J^{(2)}$ terms in (C5) correspond to the $q=0$, ±1, and ±2 terms, respectively in (C4).

The relaxation time $T_{1\rho}$ is defined in a similar manner, except we have to include the effect of the strong rf oscillating field [5e] in the spin Hamiltonian $\mathcal{H}_0$:

$$d\langle I_x+I_x'\rangle/dt=-i\langle\mathcal{H}_0(t)+\mathcal{H}_1(t),\ I_x+I_x'\rangle$$
$$=-\langle I_x+I_x'\rangle/T_{1\rho}, \qquad \text{(C6)}$$

$$\mathcal{H}_0=\omega I_z+\omega I_z'+\omega_1(I_x\cos\omega t+I_x'\cos\omega t$$
$$+I_y\sin\omega t+I_y'\sin\omega t). \qquad \text{(C7)}$$

The interaction representation for $T_{1\rho}$, which will be denoted by $\tilde{}$, is defined as $\tilde{A}(t)=U(t)AU^{-1}(t)$ where the function U is a solution of $dU/dt=iU\mathcal{H}_0(t)$, $\mathcal{H}_0$ being given by (C7); Abragam[5e] has shown that

$$U=\exp(i\omega_1 I_x t+i\omega_1 I_x' t)\exp(i\omega I_z t+i\omega I_z' t). \qquad \text{(C8)}$$

$T_{1\rho}$ is given by

$$T_{1\rho}^{-1}\langle I_x+I_x'\rangle=\sum_{q=0,\pm1,\pm2}\int_0^\infty\langle F^{(q)}F^{(-q)}(t+\tau)[\tilde{A}^{(q)}(t),[\tilde{A}^{(-q)}(t+\tau),I_x+I_x']]\rangle d\tau. \qquad \text{(C9)}$$

The * and $\tilde{}$ representations, which correspond to the rotating coordinate system and doubly rotating coordinate system,[5e] respectively, are related to each other by

$$\tilde{A}^{(q)}(t)=\exp(i\omega_1 I_x t+i\omega_1 I_x' t)A^{(q)*}(t)$$
$$\times\exp(-i\omega_1 I_x t-i\omega_1 I_x' t). \qquad \text{(C10)}$$

Now let us correlate $T_{1\rho}^{-1}$ with T_2^{-1} by comparing (C9) with (C4). The only difference is that an extra similarity transformation (C10) has been introduced to transform from the * system to the $\tilde{}$ system in addition to the original time dependence $A^{(q)*}(t)=e^{iq\omega t}A^{(q)}$. Since $\omega\gg\omega_1$, the extra time dependences introduced by (C10) for $q=\pm1$ and ±2 are quite small and negligible compared to the original time dependences $e^{\pm i\omega t}$ and $e^{\pm2i\omega t}$. Hence the $J^{(1)}$ and $J^{(2)}$ terms for $T_{1\rho}^{-1}$ and T_2^{-1} are identical.

It is then only necessary to evaluate the commutators for $q=0$ in (C9). It is convenient to transform I_x, I_y, I_z to I_x, I_+, and I_-, where $I_\pm=I_y\pm iI_z$. Thus $\tilde{I}_x(t)=I_x^*(t)$ and $\tilde{I}_\pm(t)=\exp(\pm i\omega_1 t)I_\pm^*(t)$. We may write $A^{(0)*}$ as

$$A^{(0)*}=\tfrac{1}{3}\alpha(I_x^*I_x'^*+I_y^*I_y'^*-2I_z^*I_z'^*)=A_1^{(0)*}+A_2^{(0)*},$$
$$A_1^{(0)*}=\tfrac{1}{4}\alpha(I_+^*I_+'^*+I_-^*I_-'^*),$$
$$\tilde{A}_1^{(0)}=\tfrac{1}{4}\alpha[I_+^*I_+'^*\exp(2i\omega_1 t)+I_-^*I_-'^*\exp(-2i\omega_1 t)],$$
$$A_2^{(0)*}=\tfrac{1}{12}\alpha(4I_x^*I_x'^*-I_+^*I_-'^*-I_-^*I_+'^*)=\tilde{A}_2^{(0)}.$$

It can be readily shown that $A_2^{(0)*}$ commutes with I_x+I_x'; and, furthermore, the trace of $[A_2^{(0)*},[A^{(0)},I_x+I_x']]$ is zero. The $q=0$ commutators for T_2^{-1} and $T_{1\rho}^{-1}$ are therefore given by (C11) and (C12), respectively.

$$[A^{(0)*}(t),[A^{(0)*}(t+\tau),I_x+I_x']]$$
$$=[A_1^{(0)*}(t),[A_1^{(0)*}(t+\tau),I_x+I_x']] \qquad \text{(C11)}$$

$$[\tilde{A}^{(0)}(t),[\tilde{A}^{(0)}(t+\tau),I_x+I_x']]$$
$$=[\tilde{A}_1^{(0)}(t),[\tilde{A}_1^{(0)}(t+\tau),I_x+I_x']]. \qquad \text{(C12)}$$

(C11) is time-independent. It is permissible to neglect the difference between $\exp(2i\omega_1 t)$ and $\exp(-2i\omega_1 t)$ because they give identical Fourier transforms; hence,

$$[\tilde{A}_1^{(0)}(t),[\tilde{A}_1^{(0)}(t+\tau),I_x+I_x']]$$
$$=\exp(2i\omega_1\tau)[A_1^{(0)*}(t),[A_1^{(0)*}(t+\tau),I_x+I_x']]. \qquad \text{(C13)}$$

Therefore, $T_{1\rho}^{-1}$ is given also by (C5), except that $J^{(0)}(0)$ must be replaced by $J^{(0)}(2\omega_1)$. This is the same result as that derived by Hubbard.[6b]

Similarly, for relaxation by dipolar coupling between unlike spins, $T_{1\rho}^{-1}$ are related to T_2^{-1} by replacing $J^{(0)}(0)$ with $J^{(0)}(\omega_1)$.